Title

In vivo fluorescence reflectance imaging of protease activity in a mouse model of post-traumatic osteoarthritis

Journal

Osteoarthritis and Cartilage, 22(10)

ISSN

1063-4584

Authors

Satkunananthan, PB

Anderson, MJ

De Jesus, NM

et al.

Publication Date

2014-10-01

DOI

10.1016/j.joca.2014.07.011

Peer reviewed

Published in final edited form as:
Osteoarthritis Cartilage. 2014 October ; 22(10): 1461–1469. doi:10.1016/j.joca.2014.07.011.

In Vivo Fluorescence Reflectance Imaging of Protease Activity in a Mouse Model of Post-Traumatic Osteoarthritis

Patrick B. Satkunananthan[1,2], **Matthew J. Anderson**[1], **Nicole M. De Jesus**[2,3], **Dominik R. Haudenschild**[1,2], **Crystal M. Ripplinger**[2,3], and **Blaine A. Christiansen**[1,2]

Patrick B. Satkunananthan: psatkun@ucdavis.edu; Matthew J. Anderson: mjanderson@ucdavis.edu; Nicole M. De Jesus: drhaudenschild@ucdavis.edu; Dominik R. Haudenschild: ndejesus@ucdavis.edu; Crystal M. Ripplinger: cripplinger@ucdavis.edu; Blaine A. Christiansen: bchristiansen@ucdavis.edu

[1]University of California-Davis Medical Center, Department of Orthopaedic Surgery

[2]University of California-Davis, Biomedical Engineering Graduate Group

[3]University of California-Davis Medical Center, Department of Pharmacology

Abstract

Objective—Traumatic joint injuries initiate a surge of inflammatory cytokines and proteases that may contribute to cartilage and subchondral bone degeneration. Detecting these early biological processes in animal models of post-traumatic osteoarthritis (PTOA) typically involves ex vivo analysis of blood serum or synovial fluid biomarkers, or destructive histological analysis of the joint. In this study, we used in vivo fluorescence reflectance imaging (FRI) to quantify protease activity, matrix metalloproteinase (MMP) activity, and Cathepsin K activity in mice following ACL rupture. We hypothesized that these processes would be elevated at early time points following traumatic joint injury (1–14 days), but would return to control levels at later time points (4–8 weeks).

Design—Mice were injured via tibial compression overload, and FRI imaging was performed at multiple time points from 1–56 days after injury using commercially available activatable fluorescent tracers to quantify protease activity, MMP activity, and cathepsin K activity in injured vs. uninjured knees. PTOA was assessed at 56 days post-injury using micro-computed tomography and whole-joint histology.

Results—Protease activity, MMP activity, and cathepsin K activity were all significantly increased in injured knees relative to uninjured knees at all time points, peaking at 1–7 days post-injury, then decreasing at later time points while still remaining elevated relative to controls.

Correspondence: Blaine A. Christiansen, Ph.D., UC Davis Medical Center, Department of Orthopaedic Surgery, 4635 2nd Ave, Suite 2000, Sacramento, CA 95817, Phone: 916-734-3974, Fax: 916-734-5750, bchristiansen@ucdavis.edu.

Author Contributions
All authors were fully involved in this study and in preparation of the manuscript.

Competing Interest Statement
The authors have no potential conflicts of interest to disclose.

Conclusions—This study establishes FRI imaging as a reliable method for *in vivo* quantification of early biological processes in a translatable mouse model of PTOA, and provides crucial information about the time course of inflammation and biological activity following joint injury. These data may inform future studies aimed at targeting early inflammation to reduce the development of PTOA.

Introduction

Osteoarthritis (OA) is a primary musculoskeletal health concern, affecting approximately 27 million Americans [1]. Post-traumatic osteoarthritis (PTOA) is commonly observed within 10–20 years following anterior cruciate ligament (ACL) rupture [2–4]. Traumatic joint injuries initiate a surge of inflammatory cytokines, matrix metalloproteinases (MMPs), cathepsin proteases, and other degradative enzymes that contribute to cartilage and subchondral bone degeneration [2, 5–11]. Detecting these early biological processes in animal models of OA typically involves analysis of blood serum or synovial fluid biomarkers, or destructive histological analysis of the joint. The ability to quantify these processes non-invasively *in vivo* has the distinct advantages of rapid measurement time, relatively low cost, and the capability to perform repeated longitudinal measurements in the same animals at multiple time points or following therapy. Additionally, non-invasive *in vivo* analyses preclude the possibility of exacerbated inflammation or damage to the joint as a direct result of the sampling procedure.

Near-infrared protease activatable probes combined with fluorescence reflectance imaging (FRI) have become widely used for *in vivo* imaging to visualize and quantify cellular activity. These optical tracers are fluorescently quenched until a linker domain is cleaved by a specific protease of interest, which then produces a robust fluorescent signal. These techniques have been extensively validated and used in studies of cancer [12–15] and atherosclerosis [16–19], but are also potentially useful for studies of the musculoskeletal system to measure markers of inflammation and matrix degradation (cathepsin proteases and matrix metalloproteinases (MMPs)) and bone turnover (cathepsin K), which have vital roles in OA progression. Commercially available fluorescent activatable probes have been validated for use in musculoskeletal applications [20–23]. However, no studies have utilized these methods in an animal model of PTOA to determine the dynamic protease profile following joint injury or to quantify disease severity or progression.

In this study, we used FRI to quantify the time course of biological processes associated with PTOA progression following non-invasive joint injury in mice. We hypothesized that inflammatory biomarkers and degradative processes would be elevated at early time points following traumatic joint injury (1–14 days), but would return to control levels at later time points (4–8 weeks). These results of this study reveal, for the first time, the dynamic time course of protease activity in joints following injury, and establish FRI imaging as a feasible method for *in vivo* quantification of these biological processes in a mouse model of PTOA.

Methods

Animals

A total of 54 C57BL/6 mice (27 male, 27 female; 10 weeks old at the time of injury) were obtained from Harlan Sprague Dawley, Inc. (Indianapolis, IN, USA). Forty-eight mice (24 male, 24 female) were injured using tibial compression overload, while 6 mice (3 male, 3 female) were sham injured. Animals were housed in a compliant facility at UCDMC for a 2-week acclimation period prior to injury. All animals were maintained and used in accordance with National Institutes of Health guidelines on the care and use of laboratory animals, and the study was approved by our institutional Animal Studies Committee.

Tibial compression-induced knee injury

Mice were subjected to non-invasive ACL rupture induced by a single overload cycle of tibial compression as previously described [24]. Briefly, mice were anesthetized and placed in a prone position in a materials testing system (Bose ElectroForce 3200, Eden Prairie, MN, USA) with tibial compression loading platens (Fig. 1). A single dynamic axial compressive load was applied at 1 mm/s to the right lower leg to a target compressive force of 12 N to produce ACL rupture. This loading protocol produces failure of the ACL with avulsion fracture from the distal femur [24, 25]. Contralateral limbs remained uninjured, and served as internal controls. Sham injury was performed by anesthetizing mice and loading them into the tibial compression system, then applying a 1–2 N compressive load for ~5 seconds.

Fluorescent reflectance imaging (FRI)

All mice were imaged on days 1, 3, 7, 14, 28, and 56 after injury using *in vivo* FRI to quantify levels of fluorescence from activated probes in injured knees vs. contralateral knees. Three probes were used in this study: ProSense 680, MMPSense 680, and CatK 680 FAST (Table 1; PerkinElmer, Waltham, MA). Sixteen injured mice (8 male, 8 female) were analyzed with each of the fluorescent activatable probes; 6 uninjured (sham) mice (3 male, 3 female) were analyzed with ProSense 680 in order to confirm that there were no right/left differences in uninjured mice, and to quantify possible systemic inflammation that may be measureable in contralateral limbs of injured mice. In previous studies, both MMPSense [26, 27] and ProSense [13, 16] have been shown to localize to sites of inflammation, while CatK has been demonstrated to localize to sites of increased bone resorption and osteoclast activity [28].

Before each imaging time point (24 hours prior for ProSense 680 and MMPSense 680, and 6 hours prior for CatK 680 FAST), mice were anesthetized via isoflurane inhalation, and 10 μL (~0.1 mg/kg, IV) of probe was administered to each mouse. Hair was removed with a depilatory from the ventral aspect of both legs, and mice were imaged three at a time (22.5 cm field of view) in the imaging system (IVIS Spectrum, PerkinElmer, Waltham, MA). Each mouse was imaged twice at each time point in two different positions (left, right, or center; Fig. 2A), and results from the two images were averaged for each mouse/time point. Mouse legs were positioned such that the anterior-medial aspect of the knees was horizontal to allow for even epi-illumination. The legs were taped down across the ankle, and image processing and quantification was performed via IVIS *LivingImage* software.

The excitation and emission filters for all probes were 675±35 nm and 700±35 nm, respectively, and were chosen based on the peak excitation and emission spectra of the probes (680/700 nm ex/em for ProSense 680 and MMPSense 680; 675/693 nm ex/em for CatK 680 FAST). The exposure time for each probe was 0.75 sec for ProSense 680, 0.75 sec for MMPSense 680, and 1.0 sec for CatK 680 FAST. Spatial binning of pixels was set at the Medium option and the F/Stop was set to 2. Quantification of fluorescence intensity was performed by evaluating the *total radiant efficiency* ([photons/sec]/[μW/cm^2]) of the signal within a region of interest (ROI). The ROI was a uniform circle of 12.3 mm^2 that was anatomically selected around the knee on a grayscale photograph of the mice (Fig. 2B), such that the ROI selections encapsulated the entire knee and were unbiased by the fluorescent signals. Subsequently, the total radiant efficiency of the injured knee was normalized to the contralateral uninjured knee of each mouse, to account for mouse-to-mouse variation in delivery of the fluorescent probe.

Micro-computed tomography analysis of epiphyseal trabecular bone and osteophyte formation

Injured and uninjured knees from 8 male and 8 female mice were analyzed with micro-computed tomography (μCT 35, SCANCO, Brüttisellen, Switzerland) to quantify trabecular bone structure of the distal femoral epiphysis and osteophyte formation around the joint. All mice were sacrificed 56 days post-injury following the last time point for FRI imaging. Dissected limbs were fixed in 4% paraformaldehyde for 48 hours, then preserved in 70% ethanol. Knees were scanned according to the guidelines for μCT analysis of rodent bone structure [29] (energy = 55 kVp, intensity = 114 mA, 10 μm nominal voxel size, integration time = 900 ms). Analysis of trabecular bone in the distal femoral epiphysis was performed by manually drawing contours on 2D transverse slices; the distal femoral epiphysis was delineated as the region of trabecular bone enclosed by the growth plate and subchondral cortical bone plate (Fig. 3). Using the manufacturer's analysis software, we quantified trabecular bone volume per total volume (BV/TV), trabecular thickness (Tb.Th), trabecular separation (Tb.Sp), trabecular number (Tb.N), bone tissue mineral density (Tissue BMD; mg HA/cm^3 BV), and apparent mineral density (Apparent BMD; mg HA/cm^3 TV). Osteophyte volume was calculated for each knee. For this analysis, manual contours were drawn to quantify all non-native mineralized tissue in and around the joint space, excluding naturally ossified structures (patella, fabella, anterior and posterior horns of the menisci; Fig. 3).

Whole-joint histology of articular cartilage

Following μCT imaging, knees from the same 8 male mice and 8 female mice were analyzed with whole-joint histology to quantify cartilage and joint deterioration. Knee joints were decalcified for four days in 10% buffered formic acid, and processed for standard paraffin embedding. From each joint, 4 sagittal slices of 6 μm thickness were sectioned from the medial joint, separated by 250 μm. The medial joint was analyzed since this is the primary site of joint degeneration in our previous studies, and in studies by other investigators using similar models [24, 30]. Slides were stained with Safranin-O and Fast Green in order to assess proteoglycan content, articular cartilage degeneration, and overall joint integrity. Slides were blinded and graded by three independent readers using the semi-quantitative OARSI scale [31]. Grades were assigned to the medial tibial plateau and medial femoral

condyle. Grades from the three readers were averaged for each section, and all gradable sections were averaged for each knee.

Statistical analysis

For all analyses, paired Student's t-tests were used within each experimental group in order to determine differences in injured vs. uninjured knees. Differences in FRI readings between time points were analyzed with repeated measures ANOVA. FRI, μCT, and histology data were compared between male and female mice at each time point using unpaired t-test. Differences were considered statistically significant at $p < 0.05$ for all tests. All data is presented as mean ± 95% confidence interval. We also performed a statistical analysis to assess the effect of mouse position within the imaging chamber (left, right, center). We performed repeated-measures ANOVA on radiant efficiencies of mice imaged in the three positions, by delineating both the position on the stage and the position of a mouse leg with respect to the center as additional ordinal variables.

Results

FRI quantification of protease, MMP, and cathepsin K activity

Protease activity (ProSense 680), MMP activity (MMPSense 680), and cathepsin K activity (CatK 680 FAST) were all significantly increased in the injured knee compared to the contralateral (uninjured) knee at all time points (Fig. 4–5; $p < .05$). No significant differences were observed between male and female mice for any of the probes at any of the time points examined. Uninjured mice did not exhibit significant differences between the right and left knees at any time points. No differences in protease activity (ProSense 680) were observed between uninjured mice and contralateral knees at any time points except at 14 days post-injury, at which point protease activity of uninjured mice was significantly lower than contralateral knees, and significantly lower than all other time points for uninjured mice.

Normalization of fluorescence data (injured/contralateral for each mouse) indicated that MMPSense and ProSense were elevated 33–77% from days 1–14 post-injury, then decreased at later time points while still remaining 24–37% greater than contralateral limbs until at least 56 days post-injury. Normalized data from the CatK probe exhibited a less consistent time course, with noticeable peaks in Cathepsin K activity at days 1 and 14. The raw (non-normalized) CatK 680 signal exhibited significant increases in both the injured and contralateral knees (Fig. 5), particularly at days 3 and 7 relative to other time points. Fluorescence intensity for ProSense and MMPSense of the contralateral knees also varied throughout the time course of the study, but did not exhibit the nearly 3-fold increase observed for the CatK probe at day 3.

Analysis of imaging positions within the IVIS Spectrum confirmed that there were significant differences in total radiant efficiency quantified between each of the respective positions ($p < .001$) due to slight differences in illumination intensity. To account for this, mouse position was included as a factor in all statistical analyses. Future studies will utilize only one imaging position (center) in order to eliminate this confounding factor.

Micro-computed tomography of femoral epiphysis

MicroCT analysis of injured and uninjured joints at Day 56 revealed a ~27% loss of trabecular bone volume and notable osteophyte formation in injured joints relative to uninjured joints, consistent with our previous findings [24, 25] (Fig. 6). We observed no significant difference between males and females in osteophyte formation or trabecular bone adapatation, as injured-contralateral differences in trabecular bone volume fraction (BV/TV), connectivity density (Conn.Dens), structural model index (SMI), trabecular number (Tb.N), trabecular thickness (Tb.Th), and trabecular separation (Tb.Sp) were all similar for both sexes. We did, however, observe significant differences in the absolute values of some trabecular bone parameters between male and female mice (not considering adaptation to injury). For example, males exhibited significantly higher connectivity density ($p < .001$) and trabecular number ($p < .001$) than females, while females exhibited significantly higher trabecular thickness ($p < .001$) and trabecular separation ($p < .001$) than male mice. This is consistent with previously published findings in mice [32].

Histological analysis of articular cartilage of the medial joint

Whole-joint histology of injured and uninjured knees revealed severe deterioration of articular cartilage and subchondral bone in injured knees, often including full loss of thickness and erosion of subchondral bone, representative of severe OA (Fig. 7). Degradation of cartilage often extended into the subchondral bone causing bone-to-bone contact. Osteophyte formation was also observed on the tibia and femur, along with growth of new mineralized cartilage from menisci. The anterior portion of the tibial plateau was not noticeably damaged, while the posterior tibial plateau exhibited erosion extending to the growth plate. This pattern of degeneration is similar to what we have observed at 12 and 16 weeks post injury [25]. Histological grading revealed significant differences between injured joints and uninjured control joints for both the tibial plateau ($p < .001$) and femoral condyle ($p < .001$). No significant differences were observed between male and female mice.

Discussion

In this study, we used fluorescence reflectance imaging (FRI) to visualize and quantify the time course of the biological response to traumatic joint injury in mice *in vivo* using near-infrared fluorescent activatable probes that report on protease activity, MMP activity, and cathepsin K activity. We confirmed that these processes are significantly increased in injured joints relative to uninjured joints, particularly at early time points (1–14 days post-injury), but contrary to our initial hypothesis, these processes did not return to control values at later time points. Rather, the increased protease activity observed in injured joints remained for the duration of the study (8 weeks).

This study used FRI to quantify and characterize the dynamic protease profile longitudinally in the same animals during the development of injury-induced PTOA. We were able to demonstrate that injured joints exhibited increased levels of protease activity, MMP activity, and cathepsin K activity compared to uninjured knees. ProSense 680 specifically reports on cysteine proteases such as Cathepsins B, L, and S, while CatK 680 reports specifically on Cathepsin K activity, and MMPSense reports on a family of MMPs involved in

inflammation. A role for cathepsins (excluding Cathepsin K) is well-established in osteoarthritic progression, though they may not be the prime mediators of articular cartilage deterioration or bone turnover [33–36]. Cathepsin K plays a major role in bone resorption and aggrecan degradation; it has been recognized as one of the most abundant and primary proteases in osteoclastic activity. Additionally, Cathepsin K has shown the ability to degrade type II collagen, therefore it may also be directly involved in the degradation of articular cartilage in addition to its role in osteoclast function [37]. MMPs are the primary collagenolytic enzymes of osteoarthritic cartilage; MMP-13 is extremely active and MMP-3 is thought to be a collagenase activator [33], and MMP-9 is highly responsible for initiating osteoclastic resorption by removing the collagenous layer from the bone surface before demineralization begins [38].

In this study we observed increased Cathepsin K activity at days 3 and 7 post-injury relative to other time points in both injured and contralateral knees following injury. This is consistent with our previous study [24], in which we observed a decrease in trabecular bone volume from the femoral epiphysis of both injured and contralateral knees by 7 days post-injury. Similarly, a study of injured and contralateral knees in human subjects following traumatic joint injury showed an increase in concentrations of aggrecan and cartilage oligomeric matrix protein (COMP) fragments and stromelysin-l in contralateral knees [39]. In the current study we did not observe significant increases in early protease activity or MMP activity in the contralateral knee relative to uninjured mice or later time points. However, this contralateral effect should be carefully considered for studies of OA using FRI, and future studies should more extensively utilize uninjured (sham) mice. It is common practice to use an internal control for normalizing fluorescent signals with FRI measurements, as this accounts for possible mouse-to-mouse differences in probe delivery. Systemic variations in fluorescent signal strength may be due to probe delivery, exact placement on the imaging stage, or illumination intensity. Normalizing by an internal control for each mouse can theoretically account for these systemic variations in difference in signal strength. However, taking into account the possible contralateral increases in these biological processes following an acute injury, this may not be a suitable analysis method for future studies of OA.

We did not detect any differences in PTOA development between male and female mice using any of the analysis methods in this study. It is well known that female athletes are 4–6 times more likely than male athletes to sustain an ACL rupture during exercise or sports [40–43], however studies of both humans and animal models suggest that males may have a greater tendency to develop PTOA following traumatic joint injury [44–46]. However, the specific mechanisms contributing to this sex-related disparity are unknown. In the current study we did not observe any sex-based differences in the protease profile at any of the time points. Furthermore, we did not observe any sex-based differences in articular cartilage or subchondral bone degeneration at 56 days post-injury. This may be due to examining a single time point when severe OA has already developed. An intermediate time point may be useful for detecting sex-based differences in OA progression, similar to those observed previously [45, 46].

In vivo FRI was able to detect significant differences in fluorescent signal in injured vs. contralateral knees using three different probes, however the high variability of this *in vivo* imaging technique may limit the capability to observe relatively small differences in fluorescence levels. For example, quantification of fluorescent signals using the IVIS Spectrum system exhibited large variance and a strong dependence on position of mice within the system. The IVIS Spectrum system produces a circular beam of light from the epi-illumination excitation light source above the stage. Because we imaged three mice at a time, the centrally located mouse received the most uniform illumination; whereas the mice on the left and right sides had more non-uniformity. An analysis of mouse position within the imaging system helped elucidate this issue, and by performing a repeated-measures ANOVA on radiant efficiencies on mice imaged in different positions, we confirmed that there was a significant difference in brightness between each respective position on the stage, as well as the position of each leg, with respect to the center line. In addition, typical issues of autofluorescence and attenuation by tissue are continually a concern for *in vivo* imaging studies. In this respect, variations from mouse to mouse can make it difficult to quantify fluorescence with accuracy and reliability, as the depth of penetration of irradiated light can be considerably different. Future studies will minimize measurement variability by using only the center imaging position, however the precision of this imaging technique for detecting small differences in fluorescent signals remains unclear. However, despite these limitations, we were able to successfully track the time course of protease, MMP, and cathepsin K activity following knee injury in mice. This imaging method is non-invasive, time and cost effective, and provides longitudinal data from individual mice at multiple time points. In this way, FRI is a meaningful step forward for quantification of early biological processes in mouse models of PTOA.

This study is also somewhat limited because we did not validate our *in vivo* fluorescent signals with a histological “gold standard” such as immunohistochemistry or *in situ* hybridization. Therefore, we are unable to attribute the observed fluorescent signals to specific tissues associated with PTOA development. However, each of these fluorescent activatable probes has been extensively validated and compared to histological standards [12–19], and in particular have been validated for studies of musculoskeletal tissues [20–23], therefore we are confident that the fluorescent signals are indicative of cellular processes at the level of the whole joint. Our future studies will utilize histological techniques to further characterize the specific tissues in which these fluorescent signals originate following traumatic joint injury using this animal model.

Using commercially available fluorescent agents we were able to quantify the time course of protease activity, MMP activity, and cathepsin K activity following traumatic injury to the ACL, with noticeable peaks at early time points (1–7 days post-injury). This early response may point to a “window of opportunity” in which treatments may be administered to most efficiently stall the progression of OA. Cathepsin and MMP inhibitors have both been utilized experimentally, both in the molecular and transcriptional pathways, as potential therapies for hindering OA progression [33]. Future studies could investigate effective time periods for treatment in the murine model, which can then be extrapolated into larger animal models and human subjects.

Conclusions

Using *in vivo* FRI, we observed substantial increases in protease activity, MMP activity, and cathepsin K activity in injured joints compared to uninjured joints in mice following traumatic knee injury. We successfully described the dynamic protease profile following joint injury, and established FRI as a useful analysis method contributing to the quantification of OA progression in mice. This study provides crucial information about the time course of inflammation and cellular activity in a translatable mouse model of knee injury, and may inform future studies aimed at targeting early inflammation to reduce the development of PTOA.

Acknowledgments

We would like to acknowledge Susan Stover and David Fyhrie for their meaningful contributions to this study.

Role of Funding Sources

Research reported in this publication was supported by the National Institute of Arthritis and Musculoskeletal and Skin Diseases, part of the National Institutes of Health, under Award Number AR062603 (BAC) and AR063348 (DRH). The content is solely the responsibility of the authors and does not necessarily represent the official views of the National Institutes of Health

References

1. Lawrence RC, Felson DT, Helmick CG, Arnold LM, Choi H, Deyo RA, et al. Estimates of the prevalence of arthritis and other rheumatic conditions in the United States. Part II. Arthritis Rheum. 2008; 58:26–35. [PubMed: 18163497]
2. Lohmander LS, Englund PM, Dahl LL, Roos EM. The long-term consequence of anterior cruciate ligament and meniscus injuries: osteoarthritis. Am J Sports Med. 2007; 35:1756–1769. [PubMed: 17761605]
3. Gillquist J, Messner K. Anterior cruciate ligament reconstruction and the long-term incidence of gonarthrosis. Sports Med. 1999; 27:143–156. [PubMed: 10222538]
4. Myklebust G, Bahr R. Return to play guidelines after anterior cruciate ligament surgery. Br J Sports Med. 2005; 39:127–131. [PubMed: 15728687]
5. Madry H, Luyten FP, Facchini A. Biological aspects of early osteoarthritis. Knee Surg Sports Traumatol Arthrosc. 2012; 20:407–422. [PubMed: 22009557]
6. Goldring MB, Goldring SR. Osteoarthritis. Journal of Cellular Physiology. 2007; 213:626–634. [PubMed: 17786965]
7. Anderson DD, Chubinskaya S, Guilak F, Martin JA, Oegema TR, Olson SA, et al. Post-traumatic osteoarthritis: Improved understanding and opportunities for early intervention. J Orthop Res. 2011; 29:802–809. [PubMed: 21520254]
8. Kurz B, Lemke AK, Fay J, Pufe T, Grodzinsky AJ, Schunke M. Pathomechanisms of cartilage destruction by mechanical injury. Ann Anat. 2005; 187:473–485. [PubMed: 16320827]
9. Fitzgerald JB, Jin M, Dean D, Wood DJ, Zheng MH, Grodzinsky AJ. Mechanical compression of cartilage explants induces multiple time-dependent gene expression patterns and involves intracellular calcium and cyclic AMP. J Biol Chem. 2004; 279:19502–19511. [PubMed: 14960571]
10. Brophy RH, Rai MF, Zhang Z, Torgomyan A, Sandell LJ. Molecular analysis of age and sex-related gene expression in meniscal tears with and without a concomitant anterior cruciate ligament tear. J Bone Joint Surg Am. 2012; 94:385–393. [PubMed: 22362494]
11. Irie K, Uchiyama E, Iwaso H. Intraarticular inflammatory cytokines in acute anterior cruciate ligament injured knee. Knee. 2003; 10:93–96. [PubMed: 12649034]

12. Zhang H, Morgan D, Cecil G, Burkholder A, Ramocki N, Scull B, et al. Biochromoendoscopy: molecular imaging with capsule endoscopy for detection of adenomas of the GI tract. Gastrointest Endosc. 2008; 68:520–527. [PubMed: 18499106]
13. Gounaris E, Tung CH, Restaino C, Maehr R, Kohler R, Joyce JA, et al. Live imaging of cysteine-cathepsin activity reveals dynamics of focal inflammation, angiogenesis, and polyp growth. PLoS One. 2008; 3:e2916. [PubMed: 18698347]
14. Sheth RA, Mahmood U. Optical molecular imaging and its emerging role in colorectal cancer. Am J Physiol Gastrointest Liver Physiol. 2010; 299:G807–820. [PubMed: 20595618]
15. Clapper ML, Hensley HH, Chang WC, Devarajan K, Nguyen MT, Cooper HS. Detection of colorectal adenomas using a bioactivatable probe specific for matrix metalloproteinase activity. Neoplasia. 2011; 13:685–691. [PubMed: 21847360]
16. Nahrendorf M, Sosnovik DE, Waterman P, Swirski FK, Pande AN, Aikawa E, et al. Dual channel optical tomographic imaging of leukocyte recruitment and protease activity in the healing myocardial infarct. Circ Res. 2007; 100:1218–1225. [PubMed: 17379832]
17. Jaffer FA, Kim DE, Quinti L, Tung CH, Aikawa E, Pande AN, et al. Optical visualization of cathepsin K activity in atherosclerosis with a novel, protease-activatable fluorescence sensor. Circulation. 2007; 115:2292–2298. [PubMed: 17420353]
18. Jaffer FA, Libby P, Weissleder R. Optical and multimodality molecular imaging: insights into atherosclerosis. Arterioscler Thromb Vasc Biol. 2009; 29:1017–1024. [PubMed: 19359659]
19. Razansky D, Harlaar NJ, Hillebrands JL, Taruttis A, Herzog E, Zeebregts CJ, et al. Multispectral optoacoustic tomography of matrix metalloproteinase activity in vulnerable human carotid plaques. Mol Imaging Biol. 2012; 14:277–285. [PubMed: 21720908]
20. Kozloff KM, Quinti L, Patntirapong S, Hauschka PV, Tung CH, Weissleder R, et al. Non-invasive optical detection of cathepsin K-mediated fluorescence reveals osteoclast activity in vitro and in vivo. Bone. 2009; 44:190–198. [PubMed: 19007918]
21. Kozloff KM, Quinti L, Tung C, Weissleder R, Mahmood U. Non-invasive imaging of osteoclast activity via near-infrared cathepsin-K activatable optical probe. J Musculoskelet Neuronal Interact. 2006; 6:353. [PubMed: 17185820]
22. Kozloff KM, Volakis LI, Marini JC, Caird MS. Near-infrared fluorescent probe traces bisphosphonate delivery and retention in vivo. J Bone Miner Res. 2010; 25:1748–1758. [PubMed: 20200982]
23. Kozloff KM, Weissleder R, Mahmood U. Noninvasive optical detection of bone mineral. J Bone Miner Res. 2007; 22:1208–1216. [PubMed: 17488196]
24. Christiansen BA, Anderson MJ, Lee CA, Williams JC, Yik JH, Haudenschild DR. Musculoskeletal changes following non-invasive knee injury using a novel mouse model of post-traumatic osteoarthritis. Osteoarthritis Cartilage. 2012; 20:773–782. [PubMed: 22531459]
25. Lockwood KA, Chu BT, Anderson MJ, Haudenschild DR, Christiansen BA. Comparison of loading rate-dependent injury modes in a murine model of post-traumatic osteoarthritis. J Orthop Res. 2013; 32:79–88. [PubMed: 24019199]
26. Barber PA, Rushforth D, Agrawal S, Tuor UI. Infrared optical imaging of matrix metalloproteinases (MMPs) up regulation following ischemia reperfusion is ameliorated by hypothermia. BMC Neurosci. 2012; 13:76. [PubMed: 22742423]
27. Liu N, Shang J, Tian F, Nishi H, Abe K. In vivo optical imaging for evaluating the efficacy of edaravone after transient cerebral ischemia in mice. Brain Res. 2011; 1397:66–75. [PubMed: 21571257]
28. Hoff BA, Chughtai K, Jeon YH, Kozloff K, Galban S, Rehemtulla A, et al. Multimodality imaging of tumor and bone response in a mouse model of bony metastasis. Transl Oncol. 2012; 5:415–421. [PubMed: 23323156]
29. Bouxsein ML, Boyd SK, Christiansen BA, Guldberg RE, Jepsen KJ, Muller R. Guidelines for assessment of bone microstructure in rodents using micro-computed tomography. J Bone Miner Res. 2010; 25:1468–1486. [PubMed: 20533309]
30. Glasson SS, Blanchet TJ, Morris EA. The surgical destabilization of the medial meniscus (DMM) model of osteoarthritis in the 129/SvEv mouse. Osteoarthritis Cartilage. 2007; 15:1061–1069. [PubMed: 17470400]

31. Glasson SS, Chambers MG, Van Den Berg WB, Little CB. The OARSI histopathology initiative - recommendations for histological assessments of osteoarthritis in the mouse. Osteoarthritis Cartilage. 2010; 18 (Suppl 3):S17–23. [PubMed: 20864019]
32. Glatt V, Canalis E, Stadmeyer L, Bouxsein ML. Age-related changes in trabecular architecture differ in female and male C57BL/6J mice. J Bone Miner Res. 2007; 22:1197–1207. [PubMed: 17488199]
33. Troeberg L, Nagase H. Proteases involved in cartilage matrix degradation in osteoarthritis. Biochim Biophys Acta. 2012; 1824:133–145. [PubMed: 21777704]
34. Woessner JF Jr. Purification of cathepsin D from cartilage and uterus and its action on the protein-polysaccharide complex of cartilage. J Biol Chem. 1973; 248:1634–1642. [PubMed: 4266584]
35. Fosang AJ, Neame PJ, Last K, Hardingham TE, Murphy G, Hamilton JA. The interglobular domain of cartilage aggrecan is cleaved by PUMP, gelatinases, and cathepsin B. J Biol Chem. 1992; 267:19470–19474. [PubMed: 1326552]
36. Hembry RM, Knight CG, Dingle JT, Barrett AJ. Evidence that extracellular cathepsin D is not responsible for the resorption of cartilage matrix in culture. Biochim Biophys Acta. 1982; 714:307–312. [PubMed: 6799007]
37. Dejica VM, Mort JS, Laverty S, Antoniou J, Zukor DJ, Tanzer M, et al. Increased type II collagen cleavage by cathepsin K and collagenase activities with aging and osteoarthritis in human articular cartilage. Arthritis Res Ther. 2012; 14:R113. [PubMed: 22584047]
38. Logar DB, Komadina R, Prezelj J, Ostanek B, Trost Z, Marc J. Expression of bone resorption genes in osteoarthritis and in osteoporosis. J Bone Miner Metab. 2007; 25:219–225. [PubMed: 17593491]
39. Dahlberg L, Roos H, Saxne T, Heinegard D, Lark MW, Hoerrner LA, et al. Cartilage metabolism in the injured and uninjured knee of the same patient. Ann Rheum Dis. 1994; 53:823–827. [PubMed: 7864691]
40. Arendt E, Dick R. Knee Injury Patterns among Men and Women in Collegiate Basketball and Soccer - Ncaa Data and Review of Literature. American Journal of Sports Medicine. 1995; 23:694–701. [PubMed: 8600737]
41. Powell JW, Barber-Foss KD. Sex-related injury patterns among selected high school sports. American Journal of Sports Medicine. 2000; 28:385–391. [PubMed: 10843133]
42. Hewett TE, Myer GD, Ford KR, Heidt RS Jr, Colosimo AJ, McLean SG, et al. Biomechanical measures of neuromuscular control and valgus loading of the knee predict anterior cruciate ligament injury risk in female athletes: a prospective study. Am J Sports Med. 2005; 33:492–501. [PubMed: 15722287]
43. Zelisko JA, Noble HB, Porter M. A comparison of men's and women's professional basketball injuries. Am J Sports Med. 1982; 10:297–299. [PubMed: 6814271]
44. Li RT, Lorenz S, Xu Y, Harner CD, Fu FH, Irrgang JJ. Predictors of radiographic knee osteoarthritis after anterior cruciate ligament reconstruction. Am J Sports Med. 2011; 39:2595–2603. [PubMed: 22021585]
45. van Osch GJ, van der Kraan PM, Vitters EL, Blankevoort L, van den Berg WB. Induction of osteoarthritis by intra-articular injection of collagenase in mice. Strain and sex related differences. Osteoarthritis Cartilage. 1993; 1:171–177. [PubMed: 15449423]
46. Ma HL, Blanchet TJ, Peluso D, Hopkins B, Morris EA, Glasson SS. Osteoarthritis severity is sex dependent in a surgical mouse model. Osteoarthritis Cartilage. 2007; 15:695–700. [PubMed: 17207643]

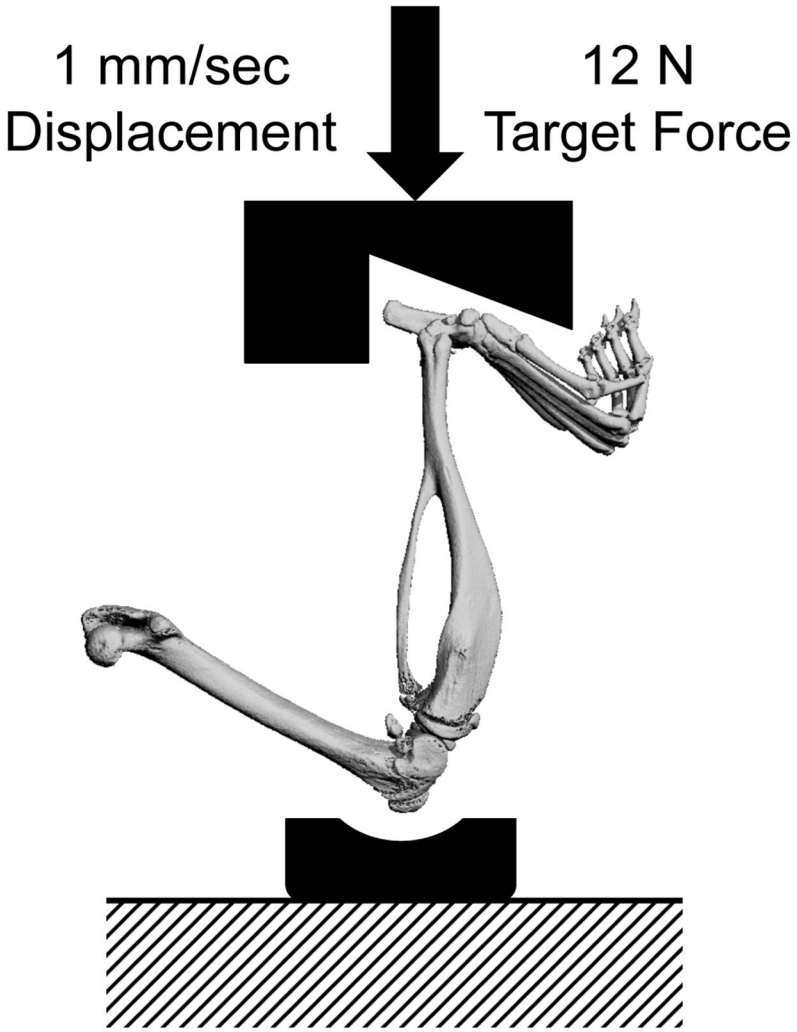

Figure 1.

Tibial compression setup for non-invasive knee injury. A single dynamic axial compressive load was applied at 1 mm/s to the right lower leg to a target compressive force of 12 N to produce ACL rupture. For uninjured mice, sham injury was performed by applying a 1–2 N compressive load.

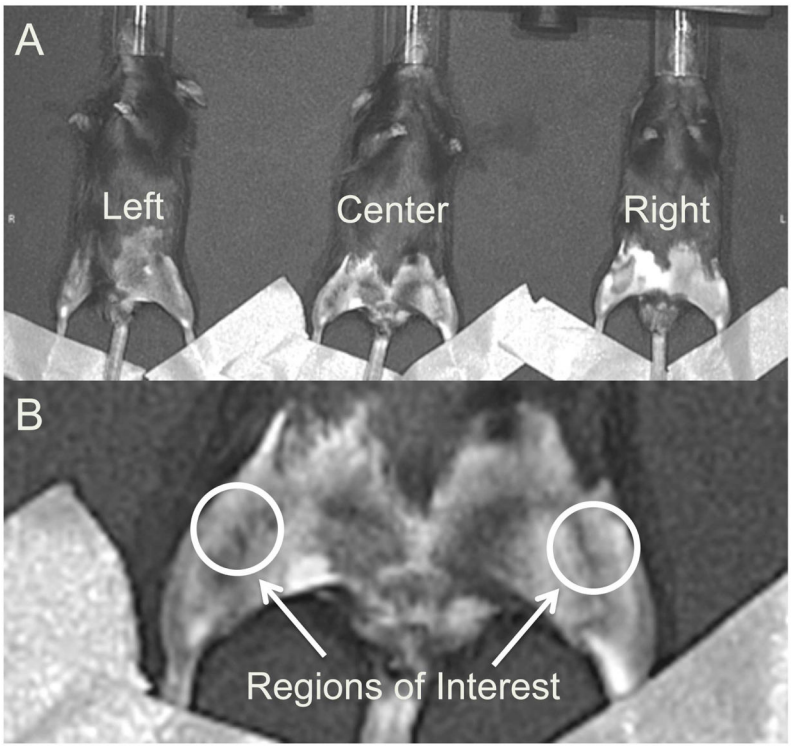

Figure 2.

(A) Imaging positions for mice in the IVIS Spectrum system. Each mouse was imaged twice at each time point in two different positions, and results from the two images were averaged for each mouse/time point. (B) Regions of interest for quantifying fluorescent signals in each knee. The region of interest was a uniform circle of 12.3 mm^2 that was anatomically selected around the knee on a grayscale photograph of the mice, such that the selection criteria were unbiased by the fluorescent signals.

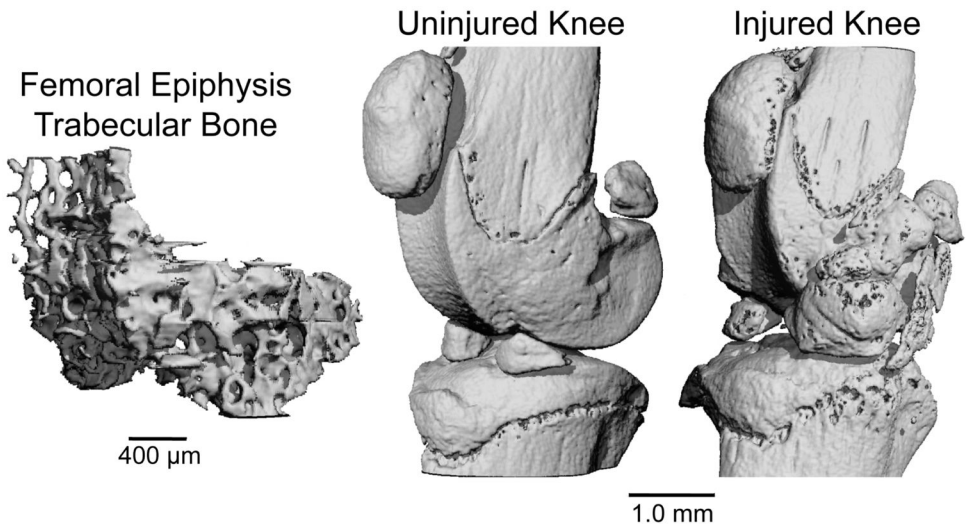

Figure 3.

(Left) Trabecular bone volume of interest from the femoral epiphysis. (Right) Uninjured and injured mouse knees at 56 days post-injury. Considerable osteophyte formation and joint degeneration are apparent on the injured knee.

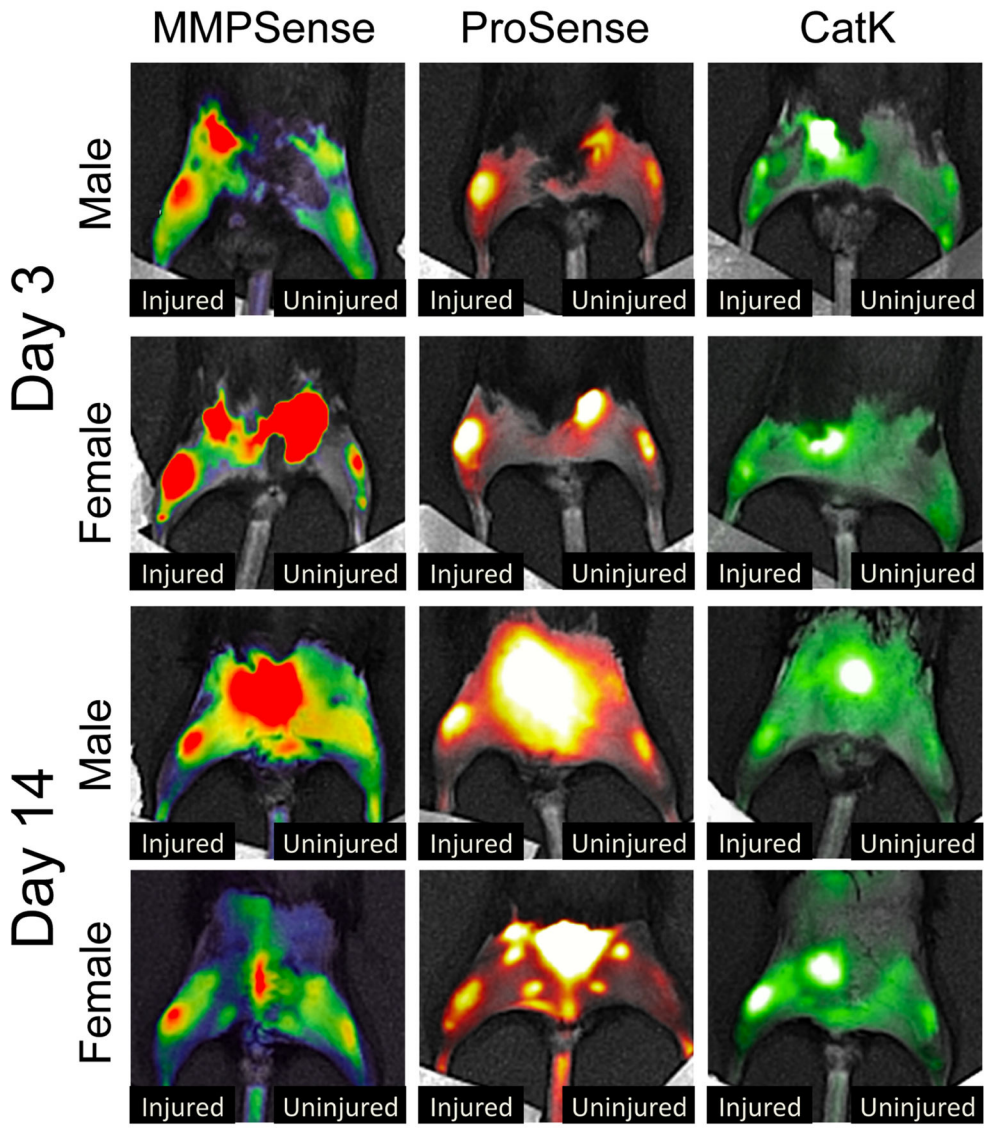

Figure 4.

Representative pseudo-colored images of male and female mice imaged with each of the fluorescent tracers at 3 and 14 days post-injury. Protease activity (ProSense 680), MMP activity (MMPSense 680), and cathepsin K activity (CatK 680 FAST) were all significantly increased in the injured knee compared to the contralateral knee at all time points.

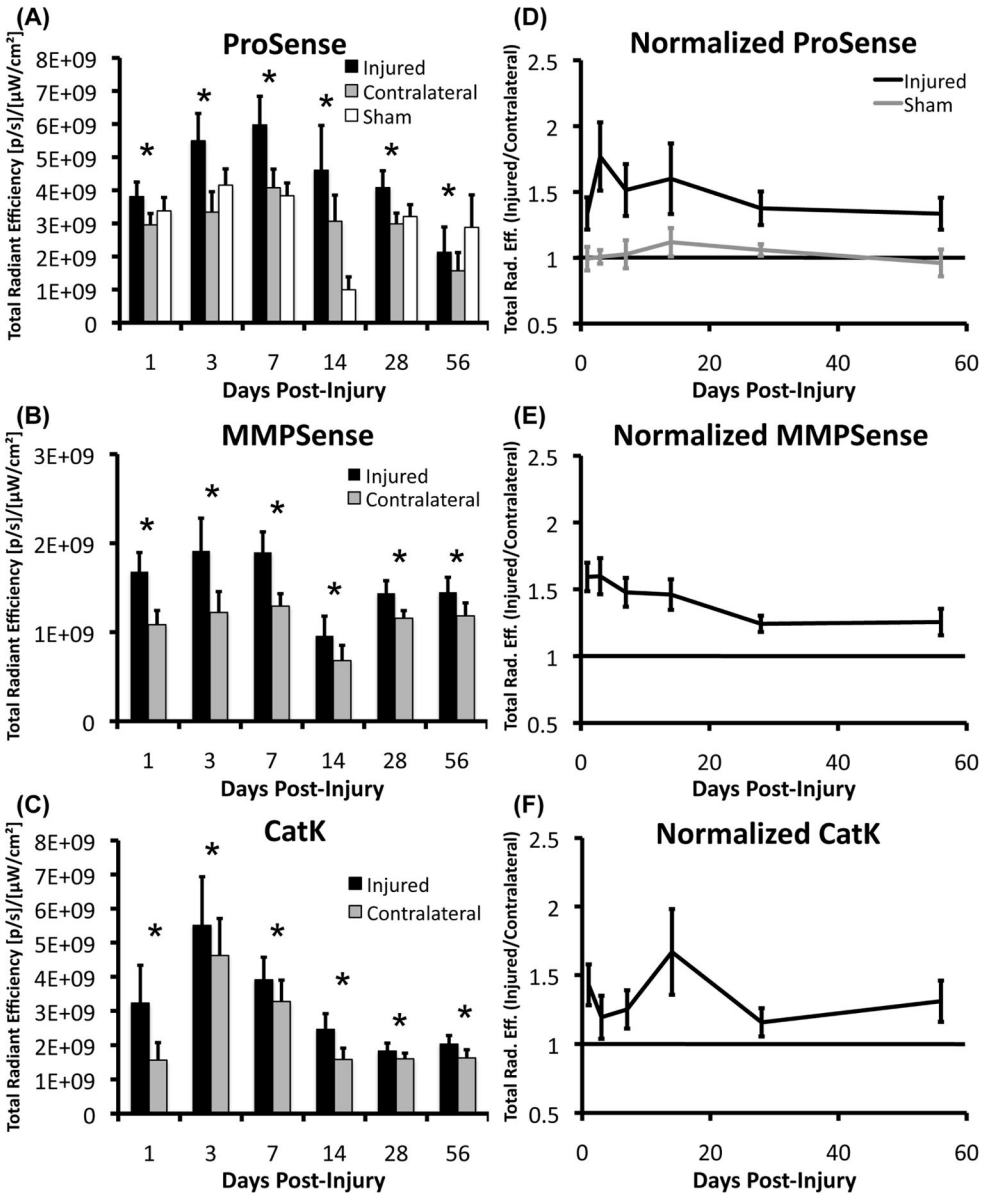

Figure 5.

(A–C) Total radiant efficiency values from each fluourescent activatable probe at each time point of interest (n = 16 mice/time point for Injured and Contralateral data, n = 6 for Sham data). (D–F) Normalized time course of total radiant efficiency (fluorescence intensity: injured knee/contralateral knee) for the three probes. Normalized fluorescence levels of MMPSense and ProSense were elevated from days 1 through 14, and decreased slightly at later time points while still remaining significantly elevated compared to uninjured limbs (above 1.0). CatK 680 FAST signals were increased in both the injured and contralateral knees at days 3–7, suggesting a systemic bone loss at these time points. All data presented as mean ± 95% confidence interval. * Injured > Contralateral ($p < 0.05$).

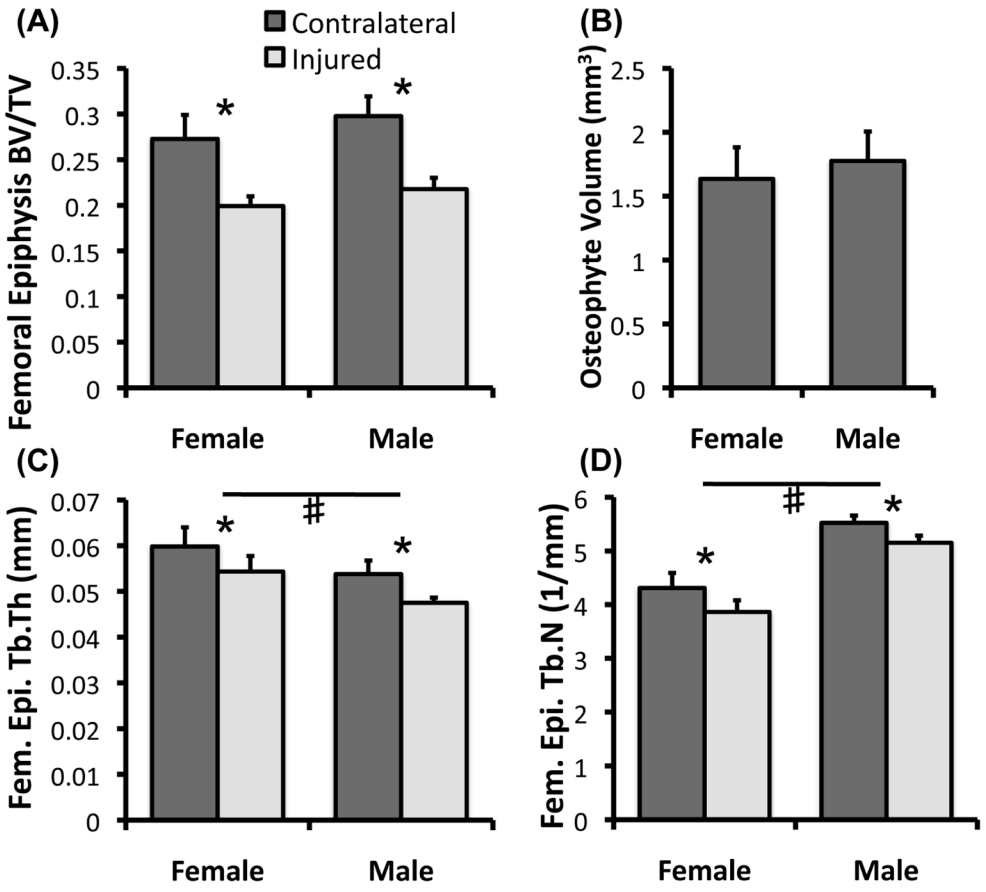

Figure 6.

(A, C, D) MicroCT analysis of femoral epiphysis trabecular bone structural parameters from injured and contralateral joints and (B) osteophyte volume of injured joints at 56 days post-injury (n = 8 mice/sex). No significant differences were observed for any parameters between males and females in adaptation to injury. All data presented as mean ± 95% confidence interval. * Injured vs. Contralateral ($p < 0.05$), # Male vs. Female ($p < 0.05$).

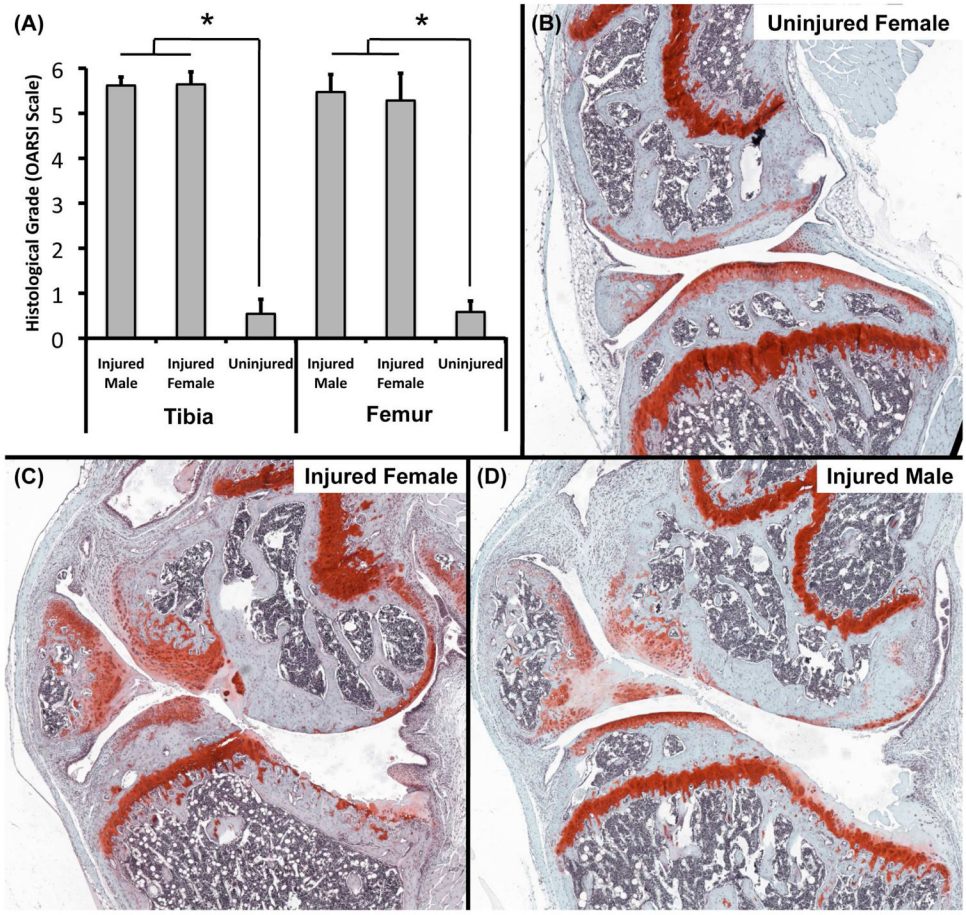

Figure 7.

Whole-joint histology of the medial aspect of injured and contralateral joints at 56 days post-injury (n = 8 mice/sex for Injured data, n = 6 mice for Uninjured data). Injured joints exhibited considerable deterioration of articular cartilage and subchondral bone, often including full loss of thickness and erosion of subchondral bone, representative of severe progressive OA (B–D). The anterior portion of the tibial plateau was not noticeably damaged, while the posterior tibial plateau exhibited erosion extended down to the growth plate. Articular cartilage grading revealed severe OA on both the tibial plateau and femoral condyle (A). No significant differences were observed between male and female mice. All data presented as mean ± 95% confidence interval. * Injured vs. Contralateral ($p < 0.05$).

Table 1

Fluorescent tracers used to quantify early processes of PTOA.

Imaging Agent	Action	Indication
MMPSense 680	Activated by matrix metalloproteinases (MMPs) including MMP-2, -3, -9, -13	Localizes to inflammatory infiltrates involved in the degradation of collagens
ProSense 680	Activated by proteases such as Cathepsin B, L, S and Plasmin	Activated by family of lysosomal cathepsin proteases, allows detection of activated macrophages, neutrophils, eosinophils in the inflammatory response
CatK 680 FAST	Activated by Cathepsin K proteinase (Cat K)	Specific indicator of bone resorption